Journal of Chromatography, 484 (1989) 61–82
Elsevier Science Publishers B.V., Amsterdam — Printed in The Netherlands

CHROM. 22 063

STUDY OF PREPARATIVE REVERSED-PHASE CHROMATOGRAPHY BY APPLICATION OF KINETIC AND EQUILIBRIUM MODELS OF COLUMN OVERLOAD

CHARLES A. LUCY[a], JAMES L. WADE[b] and PETER W. CARR*
Department of Chemistry and Institute for Advanced Studies in Biological Process Technology, Kolthoff and Smith Halls, University of Minnesota, 207 Pleasant Street SE, Minneapolis, MN 55455 (U.S.A.)

SUMMARY

Currently, there are three fundamental models of column overload which lead to closed-form equations for the peak profile. All use some simplifying assumption(s) to make the mathematics tractable, while at the same time retaining important features of the non-linear chromatographic behavior. In this work, the kinetic model based on the work of Thomas and the equilibrium models of Houghton, and Haarhoff–Van der Linde are used to study overload processes in reversed-phase chromatography. By adjustment of the parameters, all three models can be made to closely match the experimental peak shapes under conditions of moderate overload (up to 2.5% of the column capacity), but for higher overloads the Haarhoff–Van der Linde model fails to reproduce the experimental peak shape.

All of the models involve a set of three physico-chemical parameters. These parameters are related to retention (capacity factor, k') and peak width under dilute conditions, and to the degree of isotherm overload. Experimental results show that only the parameter related to k' is essentially independent of the solute concentration and flow-rate. In principle, for all three models the peak width parameter should be independent of solute concentration, but in all cases this parameter was found to vary such that the intrinsic peak width increased with concentration. Given that all three models display this same trend, even at moderately low overloads where we feel the mathematical approximations are reasonable, we believe that the change in the peak width parameters shows an as yet unknown additional band broadening phenomenon which is related to the degree of overload and independent of flow-rate.

The solute loading capcity, in terms of the adsorption site density, can be calculated from the isotherm overload parameter. The capacity is independent of flow-rate for all three models, but only that from the kinetic model is also independent of the amount of sample loaded onto the column. The adsorption site density derived from the kinetic model for a number of different mobile phases and solutes is

[a] Present address: General Chemistry Branch, Chalk River Nuclear Laboratories, Chalk River, Ontario K0J 1J0 Canada.
[b] Present address: Hercules Research Center, Wilmington, DE 19894, U.S.A.

0021-9673/89/$03.50

consistent with results from more traditional isotherm studies. For chemically simple solutes such as the benzyl alkanols, a site density of about 3–4 μmol/m^2 was obtained.

INTRODUCTION

Interest in preparative liquid chromatography (LC) has increased rapidly over the past few years, primarily driven by the emergence of biotechnology. Together with electrophoresis, chromatography is one of the major separation methods for chemical analysis in biochemistry, but as a preparative method it stands alone due to its ability to produce a high degree of purification, coupled with little denaturation of the native molecule.

In analytical chromatography, the sample size is maintained low enough to be on the linear portion of the adsorption isotherm; consequently, retention times and band profiles are independent of concentration. In preparative chromatography, this is neither true nor desired, since sample capacity and through-put are the important figures-of-merit. Large concentrations of sample "overload" the column so that peaks become highly asymmetric, and in the case of Langmuir isotherm the peaks become tailed.

While there is a great deal of interest in preparative chromatography, there is a dearth of fundamental information. In principle, the chromatographic peaks produced under overloaded conditions contain a wealth of information about the nature of the adsorption isotherm and the band broadening processes in the column. Recently, it was shown that the ideal model of chromatography (*i.e.*, negligible axial dispersion and infinitely fast mass transfer kinetics) is very useful for the rapid determination of the adsorption isotherm[1]. However, the ideal model obviously can say nothing about the band broadening characteristics of the column. Currently there are three *closed-form* equations which can be used to generate elution profiles under non-linear chromatographic conditions: the kinetic model[2] based on the work of Thomas[3], and the equilibrium models of Houghton[4], Jaulmes *et al.*[5] and Haarhoff and Van der Linde[6]. Since it is not clear which of these three approaches is physically most realistic for the study of reversed-phase chromatography, all three models were examined.

While it is a necessary condition for the validity of a model of non-linear chromatography to accurately reproduce the skewed elution profiles, this by itself is not sufficient to "prove" that the model is valid, as has been implied by Cretier and Rocca[7]. We have shown that the Houghton model and the kinetic model can generate experimentally indistinguishable peak profiles, even under conditions such that the former does not conserve mass and yields biased values for its parameters[8]. Thus a high quality fit does not by any means indicate that a model is valid, or that the parameters are meaningful[5,8]. Rather the validity of a model can only be determined by establishing that its physico-chemical parameters have physical significance. In this work, the applicability of the kinetic, Houghton and Haarhoff–Van der Linde models to reversed-phase chromatography will be assessed by comparing the physical significance of the parameters. In addition, we hope to gain a greater understanding of the processes involved in reversed-phase chromatography by examining this mode of chromatography from the perspective of all three models.

THEORY

Giddings[9] has shown that under linear chromatographic conditions, it is possible to represent the effects of slow interphase transfer in terms of a longitudinal dispersion factor and *vice versa*. It has never been demonstrated that this equivalency holds under *non-linear chromatographic* conditions, even when the system is nearly at equilibrium. Thus there is a need to be cautious about the model used to interpret the results obtained in comparing various models of non-linear chromatography.

The differential equation that describes the mass balance in a chromatographic column is

$$\frac{\partial C}{\partial t} + u\frac{\partial C}{\partial x} + \varepsilon\frac{\partial q}{\partial t} - E\frac{\partial^2 C}{\partial x^2} = 0 \tag{1}$$

where C is the concentration of solute in the mobile phase (M), u is the chromatographic velocity (cm/s, the velocity of an unsorbed solute which explores the pores and elutes at t_0), ε is the porosity ratio which equals $(1 - \varepsilon_T)/\varepsilon_T$, where ε_T is the total porosity of the column, q is the concentration of solute in the stationary phase (M), E is the axial dispersion coefficient, x is distance (cm), and t is time (s).

A closed-form mathematicl solution of the complete non-linear chromatographic problem, as expressed in eqn. 1, is very likely impossible. A number of closed-form solutions have been obtained by neglecting one or more processes which contribute to eqn. 1, to achieve a mathematically tractable solution which preserves some of the important features of the problem.

In the *kinetic model* of column overload[2,3], axial dispersion (axial diffusion and eddy dispersion) is assumed to be negligible; that is, E is set to zero. The chromatographic mass balance under these conditions reduces to

$$\frac{\partial C}{dt} + u\frac{\partial C}{\partial x} + \varepsilon\frac{\partial q}{\partial t} = 0 \tag{2}$$

and the associated kinetic equation is

$$\frac{\partial q}{\partial t} = k_a(S_0 - q)C - k_d q \tag{3}$$

where S_0 is the concentration of binding sites (M, same units as q). Eqn. 3 is posited based on the concept that the solute forms a 1:1 complex with a fixed number of non-interacting adsorption sites on the surface of an adsorbent. At equilibrium, eqn. 3 is fully consistent with Langmuir adsorption. In contrast to the situation that prevails in affinity chromatography, in reversed-phase LC it is not clear that a solute binds to a fixed set of non-interacting sites.

The rate constants k_a and k_d are "lumped" rate parameters corresponding to solute adsorption ($M^{-1}\,s^{-1}$) and solute desorption (s^{-1}). These parameters are termed "lumped" since both chemical kinetics and solute mass transfer can contribute to them. Hiester and Vermeulen[10] have shown that the resistances to mass transfer can be

combined with the kinetic resistance of chemical adsorption under non-linear conditions when either the chemical kinetics or mass transfer clearly dominates the broadening process, or when the constant pattern condition is satisfied[10]. [In this work a large k' (*ca.* 10) was always used, which we believe justifies the constant pattern assumption[11–15].]

The solution to eqns. 2 and 3 for an impulse input has been presented previously[2] and the resultant peak profile, in dimensionless form, is

$$\frac{C}{C_0} = \left\{\frac{1 - \exp(-\gamma K C_0)}{\gamma K C_0}\right\} \left\{\frac{[\gamma(k'/y)^{\frac{1}{2}} I_1(2\gamma(k'y)^{\frac{1}{2}}) + \delta(y)]\exp[-\gamma(y + k')]}{1 - \mathrm{T}(\gamma k', \gamma y)[1 - \exp(-\gamma K C_0)]}\right\} \quad (4)$$

where $y \equiv t/t_0 - 1$; $\gamma \equiv k_d t_0$ (dimensionless rate parameter); $k' \equiv (k_a/k_d)S_0\varepsilon$ (thermodynamic k'); $K \equiv k_a/k_d$; $C_0 \equiv$ (mol of solute injected)/(column dead volume).

In the above definitions, $S_0\varepsilon$ is the maximum adsorption capacity of the column. In eqn. 4, I_1 is a first order modified Bessel function of the first kind, and the T-function is a related Bessel function integral:

$$\mathrm{T}(u,v) = \mathrm{e}^{-v} \int_0^u \mathrm{e}^{-t} I_0(\sqrt{vt})\mathrm{d}t$$

where I_0 is a zeroth order Bessel function of the first kind. The T-function acts as a switching function and produces the skew in the peak profile as the column is overloaded.

The dimensionless parameters which describe an overload peak are k', γ and KC_0. Solute retention is governed by k'; the peak width under linear chromatographic conditions is inversely related to the dimensionless rate parameter γ, and the peak skew and retention time shift due to isotherm non-linearity are reflected in the overload parameter, KC_0.

In the *equilibrium-dispersive* model of column overload based on the work of Houghton[4], it is assumed that equilibrium exists between the mobile and stationary phase at each point along the column and that axial dispersion is the dominant band broadening process. The corresponding chromatographic mass balance equation under linear conditions is

$$(1 + \varepsilon K_1)\frac{\partial C}{\partial t} + u\frac{\partial C}{\partial x} - E\frac{\partial^2 C}{\partial x^2} = 0 \quad (5)$$

In order to make eqn. 1 mathematically tractable, the isotherm is *approximated* via a parabolic relationship between q and C, and equilibrium is assumed

$$q = K_1 C + K_2 C^2 \quad (6)$$

The derivative of q with respect to t in eqn. 1 is replaced via the time derivative in eqn. 6. Note that K_1 is identical in meaning to KS_0 in the kinetic model. This type of isotherm has the advantage of being able to simulate either a convex (Langmuir) or a concave

isotherm, and so it can model either the tailing or fronting peaks resulting from column overload[5]. However, one can expect this approximation to be valid for only a small deviation from a linear isotherm[5].

Substituting the parabolic isotherm, eqn. 6, into the chromatographic mass balance, eqn. 5, and redefining variables yields the mass balance expression

$$\frac{\partial C}{\partial t} - \frac{\lambda UC}{1 + \lambda C}\frac{\partial C}{\partial \psi} - \frac{E_z}{1 + \lambda C}\frac{\partial^2 C}{\partial \psi^2} = 0 \tag{7}$$

where $U = u/(1 + K_1)$; $E_z = E/(1 + K_1)$; $\lambda = 2K_2/(1 + K_1)$; $\psi = x - Ut$.

In eqn. 7, U is the velocity that a solute band would have under linear chromatographic conditions. The parameter λ is proportional to the K_2 factor in eqn. 6. It is a measure of the non-linearity of the isotherm, and is positive for a concave and negative for a convex isotherm. The variable ψ represents the axial coordinate, z, in a reference frame moving with velocity U. The effects of axial dispersion are represented by E_z.

Eqn. 7 is a complicated non-linear partial differential equation due to the term $\lambda UC/(1 + \lambda C)$. However, if it is assumed that $|\lambda C| \ll 1$ in both denominator terms, then eqn. 7 can be solved. The resultant peak profile, written in dimensionless form, is:

$$\frac{C}{C_0} = \frac{1}{\lambda C_0}\left[\frac{4P(1 + k')}{\pi \bar{t}}\right]^{\frac{1}{2}} \frac{\exp\left[\dfrac{-(1 + k' - \bar{t})^2}{4P\bar{t}(1 + k')}\right]}{\coth\left[\dfrac{\lambda C_0}{4P(1 + k')}\right] + \operatorname{erf}\left[\dfrac{1 + k' - \bar{t}}{(4P\bar{t}[1 + k'])^{\frac{1}{2}}}\right]} \tag{8}$$

where $\bar{t} = t/t_0$ (dimensionless time); $P = E_z t_0/L^2$ (dimensionless dispersion coefficient), in which L is the length of the column. A ramification of the assumption that $|\lambda C| \ll 1$ is that the equation is restricted to very dilute solutions, or what amounts to the same thing, small non-linearities in the isotherm. Beyond this limit eqn. 8 will still closely fit experimental elution profiles, but the resultant physico-chemical parameters are biased[5,8]. The manner in which the assumption of low overload affects the peak parameters under moderate overload conditions has been discussed recently[8]. It was found that under overload conditions on a convex (Langmuir) isotherm, the peak profiles generated by eqn. 8 have a smaller area than the actual normalized peaks, and so the model is said to "lose mass". This loss of mass necessitates the inclusion of a fourth fitting parameter, a weighting factor, W, to compensate for this artifact. The mass loss has the added effect of perturbing both the effective dispersion coefficient, P, and the overload parameter, λC_0. These effects are clearly evident in the data discussed below.

An alternative equilibrium model, derived by Haarhoff and Van der Linde[6], builds on the work of Houghton, taking into account the column overload (again using a parabolic isotherm) as well as the effects of axial dispersion and lateral non-equilibrium. However, this model is not *mathematically* equivalent to the Houghton model, in contrast to what has been stated previously[16]. Based on extensive computations over a wide range in parameters, particularly at high overload, the Haarhoff–Van der Linde approach appears to conserve mass. In this work, any observed deviation of the model

was within experimental error or could be attributed to numerical inaccuracy of the computer system and algorithms employed.

In the Haarhoff–Van der Linde model, the effects of axial dispersion and lateral non-equilibrium are incorporated into a single term, the standard deviation (σ). The chromatographic mass balance is

$$\frac{\partial Q}{\partial T} - Q\frac{\partial Q}{\partial \Gamma} - \frac{1}{2}\frac{\partial^2 Q}{\partial \Gamma^2} = 0 \tag{9}$$

where Q, T and Γ are dimensionless terms related to the solute concentration, time and axial distance, respectively.

$$Q = \frac{k'YC_0}{\sigma}$$

$$T = t/t_R$$

$$\Gamma = \frac{t_R}{t_0\sigma L}\left(x - \frac{ut}{1+k'}\right)$$

In these expressions, σ is the dimensionless standard deviation for a dilute sample and Y is the isotherm parameter:

$$\sigma = \sigma_{t,C=0}/t_0 = \sigma_{v,C=0}/V_0$$

$$Y = -1/k'(\mathrm{d}^2q/\mathrm{d}C^2)_{C=0}$$

Using this treatment, the resultant dimensionless expression for the peak profile is

$$\frac{C}{C_0} = \frac{\sigma}{\sqrt{2\pi k'YC_0}}\frac{\exp(-\tau^2/2)}{\left[\dfrac{1}{\exp(k'YC_0/\sigma^2)-1}\right] + 0.5[1 + \mathrm{erf}(\tau/\sqrt{2})]} \tag{10}$$

here $\tau = (t - t_{r,C=0})/\sigma_t$ (reduced time); $k' = k'_{C=0}$ (thermodynamic k'); C_0 = (mol of solute injected)/(dead volume). The dimensionless parameters which describe the overloaded peak are k', σ and YC_0. As before, k' describes the retention of the solute under linear conditions; σ is a measure of the broadening of the peak under linear conditions, and the skewing of the peak due to column overload is governed by YC_0.

It must be understood that the above three models do not reduce to the same equation under infinitely dilute conditions. The kinetic model, with KC_0 set to zero, becomes

$$\frac{C}{C_0} = \{[\gamma(k'/y)^{\frac{1}{2}}]I_1[2\gamma(k'y)^{\frac{1}{2}}] + \delta(y)\}\exp -\gamma(y + k') \tag{11}$$

which is identical to the Giddings–Eyring kinetic-stochastic model of chromato-

graphy[17]. This equation produces assymetric peak profiles unless γ is rather large. The variance corresponding to this peak can easily be shown to be

$$\sigma^2 = 2k't_0/k_d$$

Under linear isotherm conditions, that is, λC_0 equal to zero, the Houghton equation reduces to

$$\frac{C}{C_0} = \frac{1}{2\sqrt{\pi\bar{t}P(1+k')}} \exp\left[-\frac{(1+k'-\bar{t})^2}{4P\bar{t}(1+k')}\right] \tag{12}$$

This result also exhibits peak assymetry under infinitely dilute conditions unless P is very small.

The Haarhoff–Van der Linde equation reduces to the form:

$$\frac{C}{C_0} = \frac{1}{\sqrt{2\pi\sigma}} \exp\left[\frac{-(t-t_R)^2}{2\sigma^2}\right] \tag{13}$$

This is obviously a Gaussian form.

EXPERIMENTAL

Materials and equipment

3-Phenyl-1-propanol, 4-phenyl-1-butanol, 5-phenyl-1-pentanol, *o*-cresol, 4-ethylaniline and 9-anthracenecarboxylic acid were from Aldrich (Milwaukee, WI, U.S.A.) and were used as received. 2-Phenylethanol was obtained from Sigma (St. Louis, MO, U.S.A.) and was also used as received. Triethylamine was from Aldrich and was fractionally distilled and dried before use. HPLC-grade water was obtained from a Barnstead System, HPLC-grade methanol was purchased from EM Science and HPLC-grade tetrahydrofuran was from Fisher.

The apparatus consisted of an Altex Model 110 pump (Beckman Instruments, Altex Div., San Ramon, CA, U.S.A.), a Rheodyne 7125 sampling valve (Berkeley, CA, U.S.A.) with a 100-μl loop, and a Hitatchi Model 110A UV–VIS spectrometer fit with a 20-μl high-pressure flow cell. Preliminary experiments showed that a volume of 100 μl caused no additional increase in peak width under linear isotherm conditions relative to a 10 μl injection. The linearity of the solute absorbance at the eluent concentrations was verified independently on a Varian DMS 200 UV–VIS spectrophotometer. Vydak 201THP (Sep A Ra Tions Group, Hesperia, CA, U.S.A.) (10 μm particle size; 300 Å pore size; specific surface area of the ODS material of 56 m^2/g by BET) was slurry packed into a 150 × 4.6 mm I.D. column from isopropyl alcohol at 4500 p.s.i. A long column was chosen to minimize the effects of extra column dispersion on the peak shape and width. Packing density was measured as 790 g/l. The column was thermostatted to 30.0°C using a water jacket connected to a Haake water bath. The dead time was measured using uracil [mobile phase: methanol–water (25:75)]. The corresponding dead volume was 1.92 ml.

Data were digitized and stored using an IBM Instruments Model 9000 Lab

Computer with the Chromatography Applications Program (Version 4.0, IBM Instruments). Acquisition rates were 4–40 points/s for uracil at flow-rates from 0.5 to 5.0 ml/min and from 0.25 to 2.5 points/s for retained compounds under the same conditions. All injections were made in duplicate. Raw data files for each injection were transferred to a Heath H-386 microcomputer (with a 80387 coprocessor) for subsequent analysis and fitting to eqns. 4, 8 and 10.

Prior to data fitting, the baseline (as determined by linear least-squares) was subtracted from the raw data and the time axis was normalized to the dead time of the system. The normalized data were then stored on disk for later access by the fitting programs. Each peak was represented by at least 200 points.

A randomized simplex algorithm[18] was used to fit eqns. 4, 8 and 10 to 50 data points evenly spaced across the breadth of the peak. Three parameters were used in the fitting procedure for the kinetic model (γ, k' and KC_0) and the Haarhoff–Van der Linde model (k', σ and YC_0). Four parameters were used in the fits to the Houghton model (P, k', λC_0 and a weighting factor, W). The fitting procedure was repeated at least three times on each peak, with different initial guesses, to assure that false minima were not obtained. Goodness-of-fit is reflected by the sum of the residuals, χ^2.

RESULTS AND DISCUSSION

Experimental conditions were adjusted to insure large k' values in order to minimize extra-column effects and validate the constant pattern assumption implicit in the kinetic model. Initial studies were performed with 3-phenyl-1-propanol at solute loadings ranging from those sufficiently low to be on the linear portion of the isotherm up to moderate column overload conditions (2.5% of the total capacity of the column). Fig. 1 illustrates the types of peaks observed over this range. The dots represent the experimental data points. All three models fit these peaks equally well based on χ^2, as shown in Table I, so only a single theoretical curve is shown for each peak.

There is some systematic lack of fit evident in these plots, especially at high solute loads near the leading edge of the peak. The lack of fit was not as serious, nor was it of

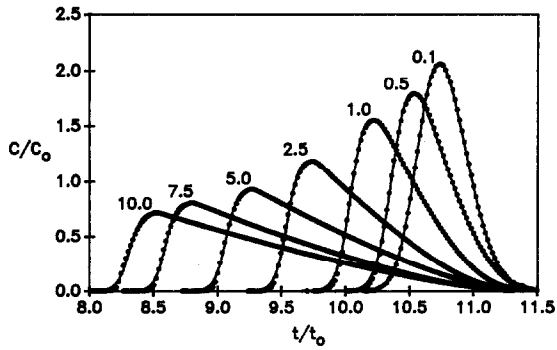

Fig. 1. Experimental elution peaks of 3-phenyl-1-propanol for various loadings. The points are the experimental data and a single curve is given for the best fit of the kinetic model. The elution profiles for the Houghton and Haarhoff–Van der Linde models are indistinguishable from the kinetic model. Experimental conditions: flow-rate, 1.0 ml/min; mobile phase, methanol–water (25:75); temperature, 30.0°C; injection volume, 100 μl. The number above each curve is the amount of solute injected in μmoles.

the same type, as previously observed in modeling high-performance affinity chromatography[2]. At this point, it does not concern us nearly so much as other complexities described below. We hypothesize that it is due to the effect of extra-column dispersion acting to broaden the nearly vertical rise in concentration from the baseline. Nevertheless, all three models can effectively match the experimental peak profiles. However, the quality of the fitting does not "prove" that the models are valid, or that the physico-chemical parameters derived from the fits are meaningful[5,8]. Rather, as stated above, the models must be judged on the basis of the physical significance of physico-chemical parameters determined in the fitting of the models to the experimental peaks. In this work, the physical significance of the parameters was probed by varying the amount of solute injected and the flow-rate. Table I shows the physico-chemical parameters extracted from chromatographic peaks resulting from trace to moderate overloads of a reversed-phase column using 3-phenyl-1-propanol as the test solute. Table II shows the physico-chemical parameters determined for a linear chromatographic peak (0.1 μmol injected) and a moderately overloaded peak (10 μmol) at flow-rates ranging from 0.5 to 5.0 ml/min.

Thermodynamic k'

In all models, the thermodynamic k' refers to the extent of solute retention expected under linear chromatographic conditions; it should be independent of concentration. Under all conditions studied, the k' extracted from each peak by all three models are comparable. Replicate injections under a variety of circumstances showed that k' is reproducible to ± 0.01. The k' did not remain absolutely constant as the solute loading increased (Table I); rather it decreased slightly. Nevertheless, no assumptions as to the significance of this trend will be made since in previous studies of preparative reversed-phase chromatography using the Houghton equilibrium-dispersive model, k' was observed to increase, decrease or remain constant depending on the chromatographic conditions[5,19].

Changes in the flow-rate had no significant effect on k', as can be seen in Table II. (The shift in k' between the 1.0 and 4.0 ml/min studies in Table I is a result of a minor change in the mobile phase composition.)

We conclude that all three models recover the k' accurately; it is not dependent on either the amount of solute injected or flow-rate.

Peak width parameters

The dimensionless rate parameter γ of the kinetic model, the dimensionless dispersion coefficient P of the equilibrium-dispersive model and the dimensionless standard deviation σ of the Haarhoff–Van der Linde model all reflect the peak width resulting from a broadening process other than overloading, in essence, the broadening of the solute band under linear chromatographic conditions. The peak width is inversely related to γ, and linearly related to P and to the square of σ.

Effect of sample loading. Table I shows the three peak width parameters obtained from the peak profiles with 0.049–9.87 μmol of 3-phenyl-1-propanol. All of the chromatographic peak width parameters change significantly as the solute loading increases. At 1.0 ml/min, γ decreased 3.8-fold, P increased 4.8-fold and σ^2 increased 2.9-fold. Similar, although smaller, trends are evident for the 4.0 ml/min data also presented in Table I. Analogous results were obtained in earlier studies of preparative

TABLE I

INFLUENCE OF SAMPLE LOADING ON THE PARAMETERS OF THE KINETIC, HOUGHTON EQUILIBRIUM-DISPERSIVE AND HAARHOFF–VAN DER LINDE MODELS FOR COLUMN OVERLOAD

Conditions: column, 150 × 4.6 mm I.D. C_{18} Vydak 201TPB; mobile phase, methanol–water (25:75); sample, 3-phenyl-1-propanol; injection volume, 100 µl and column temperature, 30.0°C.

Flow-rate (ml/min)	*µmol injected*	*Kinetic model*				*Equilibrium-dispersive model*					*Haarhoff–Van der Linde model*			
		k'	*γ*	*K* (M^{-1})	χ^2 (× 10^3)	*k'*	*P* (× 10^4)	*λ* (M^{-1})	*W*	χ^2 (× 10^3)	*k'*	*σ*	*Y*	χ^2 (× 10^3)
1.0[a]	0.049	9.94	520	82.6	7.5	9.92	1.61	−137	1.004	7.2	9.93	0.193	165	8.7
	0.099	9.88	535	61.1	4.1	9.86	1.58	−103	1.006	4.3	9.89	0.191	142	7.3
	0.49	9.90	450	40.7	11.8	9.90	1.88	−77.0	1.018	8.8	9.92	0.202	84	9.9
	0.99	9.83	385	39.2	9.7	9.82	2.30	−73.2	1.027	9.5	9.84	0.216	76	9.3
	2.47	9.80	275	37.2	7.2	9.78	3.38	−70.5	1.044	8.4	9.78	0.250	69	7.1
	4.94	9.80	200	36.4	5.1	9.79	4.90	−71.3	1.066	5.7	9.77	0.286	64	5.2
	7.40	9.72	165	36.3	4.2	9.70	6.10	−72.4	1.082	6.1	9.68	0.301	61	4.7
	9.87	9.76	135	36.0	4.3	9.74	7.70	−73.2	1.096	5.3	9.68	0.328	59	3.7
4.0[b]	0.049	9.66	310	78.8	13.0	9.65	2.74	−140	0.996	11.6	9.67	0.249	187	15.2
	0.099	9.65	305	55.2	4.6	9.65	2.80	−104	1.006	2.8	9.66	0.250	135	3.8
	0.49	9.62	300	42.9	5.9	9.63	2.86	−78.6	1.006	3.8	9.66	0.245	92	7.2
	0.99	9.70	285	42.0	4.3	9.68	3.10	−75.8	1.015	3.4	9.70	0.252	81	7.5
	2.47	9.62	235	39.5	3.8	9.62	3.90	−74.1	1.036	3.1	9.62	0.268	73	7.7
	4.94	9.59	180	38.2	3.8	9.56	5.65	−73.3	1.061	4.2	9.56	0.300	67	5.1
	7.40	9.57	165	37.1	0.8	9.55	6.10	−73.4	1.076	1.2	9.50	0.305	62	4.6
	9.87	9.58	134	37.1	2.6	9.55	8.00	−74.9	1.093	2.1	9.48	0.332	60	4.5

[a] t_0 = 108.9 s.
[b] t_0 = 27.45 s.

TABLE II

INFLUENCE OF FLOW-RATE ON THE PARAMETERS OF THE KINETIC, THE HOUGHTON EQUILIBRIUM-DISPERSIVE MODELS AND THE HAARHOFF–VAN DER LINDE MODELS

Conditions: column, 150 × 4.6 mm I.D. C_{18} Vydak 201TPB; mobile phase, methanol–water (25:75); sample, 3-phenyl-1-propanol; injection volume, 100 μl and column temperature, 30.0°C.

μmol injected	Flow-rate (ml/min)	Kinetic model				Equilibrium-dispersive model					Haarhoff–Van der Linde model			
		k'	γ	$K\ (M^{-1})$	$\chi^2\ (\times 10^3)$	k'	$P\ (\times 10^4)$	$\lambda\ (M^{-1})$	W	$\chi^2\ (\times 10^3)$	k'	σ	$Y\ (M^{-1})$	$\chi^2\ (\times 10^3)$
0.099	0.50	9.90	415	62	6.4	9.89	2.00	−98	0.997	4.7	9.91	0.217	130	7.4
	1.0	10.01	365	83	8.2	10.01	2.25	−143	0.998	6.1	10.03	0.232	180	9.3
	2.0	9.95	305	88	9.5	9.94	2.70	−159	0.995	6.8	9.97	0.253	210	10.0
	3.0	9.96	265	98	10.0	9.92	3.10	−125	0.991	7.0	9.96	0.271	200	10.0
	4.0	9.94	240	109	9.1	9.93	3.50	−178	0.995	5.6	9.95	0.286	230	8.4
	5.0	9.85	225	114	11.7	9.84	3.70	−199	0.993	7.8	9.85	0.293	250	12.5
9.87	0.50	9.73	110	37.1	2.8	9.70	9.45	−75.0	1.091	3.5	9.65	0.362	61.1	4.7
	1.0	9.78	100	38.4	3.2	9.75	10.30	−76.9	1.087	3.5	9.72	0.387	63.3	4.8
	2.0	9.85	105	39.7	1.1	9.82	9.60	−80.2	1.090	1.5	9.76	0.378	64.9	3.7
	3.0	9.74	105	38.5	1.0	9.71	9.75	−77.4	1.087	1.5	9.67	0.374	63.3	3.0
	4.0	9.85	95	39.7	1.5	9.82	10.90	−80.3	1.091	2.3	9.78	0.401	65.3	1.7
	5.0	9.70	90	38.8	2.4	9.66	11.55	−77.8	1.086	3.0	9.63	0.409	64.3	3.7

reversed-phase chromatography using the Houghton equilibrium-dispersive model[5,19]. Thus, regardless of the model adopted, the peak width parameter for all three models changes in a manner indicative of an increase in the intrinsic peak width as the solute loading increases.

However, all of the models were derived such that the peak width parameters should be independent of the degree of column overload, and so in essence, all three models have failed. However, the cause of this failure, whether it is due to flawed initial assumptions or rather due to the incompleteness of our fundamental understanding of non-linear chromatography, is unclear.

It is obvious that at the higher levels of column overload studied herein, the Houghton and Haarhoff–Van der Linde models are invalid. Both models utilize a parabolic approximation for the isotherm which is only reasonable under linear or low overload conditions. In addition, the Houghton model makes a further explicit assumption of low overload conditions ($1 + \lambda C \approx 1$). Thus, it could be argued that the results of these models, under high overload conditions, should be ignored. We are then left solely with the results for the kinetic model where γ decreases with increasing overload, which theoretically it ought not do. Based on this line of argument, the only reasonable conclusion is that the kinetic model fails to predict the details of band broadening in preparative reversed-phase chromatography.

This failure most likely results from the widely held concept that mechanical dispersion (axial diffusion and eddy dispersion) is the dominant form of band broadening in reversed-phase chromatography, as can be seen in the plot of H *vs.* u under analytical conditions, open circles in Fig. 2. At 1.0 ml/min, almost 80% of the band broadening is due to dispersion. Although Giddings has shown that dispersion effects can be represented in terms of slow interphase transfer under linear conditions, it is not known whether this equivalency is valid under non-linear conditions. If it is accepted that the kinetic model has failed, this indicates that the equivalency between dispersion and slow interphase kinetics has also failed under non-linear chromatographic conditions.

However, one point which we neglected in the above argument is that the

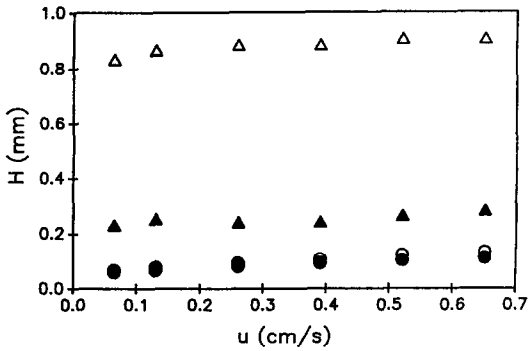

Fig. 2. H–u curves for analytical (○, ●) and overloaded (△, ▲) conditions. Open symbols are the observed plate heights and filled symbols represent H_{linear} calculated using eqn. 15 based on the kinetic model. Experimental conditions: flow-rate, 0.5–5.0 ml/min; mobile phase, methanol–water (25:75); temperature, 30.0°C; injection volume, 100 μl; sample, 3-phenyl-1-propanol; loading 0.099 (analytical) and 9.87 (overloaded) μmoles.

Houghton and Haarhoff–Van der Linde models *are* valid under linear and low overload conditions. Therefore, under these conditions, the peak width parameters of these models should not vary with solute loading. However, Jaulmes *et al.*[5], using the Houghton model, found that their dispersion parameter increased over two-fold under overload conditions for which they predicted the model to be valid (*i.e.*, $\lambda C_{max} < 0.05$). We observe variations in P and σ and λC_{max} values which are smaller than the range of validity of the parabolic isotherm approximation. Thus, the variation in the peak width parameter may not be solely an artifact of mathematical failure of the models.

Fig. 3 shows the relationship between the peak width parameters from the three models over the full range of overload studied. The terms $1/\gamma$, P and σ^2 are all directly related to the peak width. What is seen in this figure is that in comparing the kinetic with either the Haarhoff–Van der Linde or Houghton models, the linear relationship established between the terms of the two models under the low overload conditions (see the lines in Fig. 3) is continued throughout the concentration range studied. The deviation at higher overload conditions for P *vs.* $1/\gamma$ results from the "loss of mass" of the Houghton model[8], and is in any case minor compared to the change in P already predicted from the low overload conditions. Furthermore, it would be expected that the relationship between γ *vs.* P and σ would change as the degree of overload was increased since the Houghton and Haarhoff–Van der Linde models fail for mathematical reasons, whereas, using the argument above, the kinetic model should fail as a result of fundamental physical flaws in the model. However, no such break in the relationship between the peak width parameters of the kinetic model and the equilibrium-dispersive models is evident, even at the higher concentrations where the parabolic isotherm assumption perturbs the overload parameters (Fig. 4).

Thus, since all three models display the same trend of increasing intrinsic peak width as the overload increases, we believe that there must be an underlying physical cause, separate from the assumptions of each individual model, which is responsible. That is, the models are believed to fail, not due to invalid assumptions, but rather due to *incompleteness*. We have a number of speculations as to the origin of this "additional" band broadening process, but at this time we are not able to devise a definitive experiment.

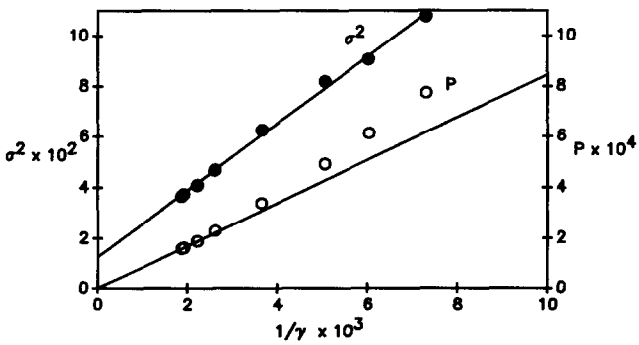

Fig. 3. Relationship between peak width parameters for injections of 0.049 (linear conditions) to 9.87 (moderate overload) μmol of 3-phenyl-1-propanol. Open circles indicate P plotted *versus* $1/\gamma$ and solid circles are σ^2 *vs.* $1/\gamma$. Lines are the extrapolation of the relationship between the peak width parameters under load overload conditions (*i.e.*, lowest values of $1/\gamma$). Conditions are as stated in Table I.

TABLE III

MODEL PARAMETERS FOR INJECTIONS OF 9-ANTHRACENECARBOXYLIC ACID

Conditions: column, 150 × 4.6 mm I.D. C_{18} Vydak 201TPB; mobile phase, methanol–0.01 *M* phosphate buffer, pH 6.8 (20:80); flow-rate, 1.0 ml/min; injection volume, 100 μl and column temperature, 30.0°C.

μmol injected	*Kinetic model*				*Equilibrium-dispersive model*					*Haarhoff–Van der Linde model*			
	k'	γ	$K\ (M^{-1})$	$\chi^2\ (\times 10^3)$	k'	$P\ (\times 10^4)$	$\lambda\ (M^{-1})$	W	$\chi^2\ (\times 10^3)$	k'	σ	$Y\ (M^{-1})$	$\chi^2\ (\times 10^3)$
0.02	12.30	340	820	8.4	12.29	2.1	−1480	1.008	10.2	12.31	0.264	1700	10.0
0.20	12.21	160	850	2.6	12.19	4.8	−1670	1.050	2.7	12.10	0.358	1540	3.8
2.01	11.70	43	690	1.4	11.66	24.0	−1570	1.178	1.0	–	–	–	7.7[a]

[a] Haarhoff–Van der Linde model could not satisfactorally fit this peak, as evidenced by χ^2 being 6–7 times that of the other models.

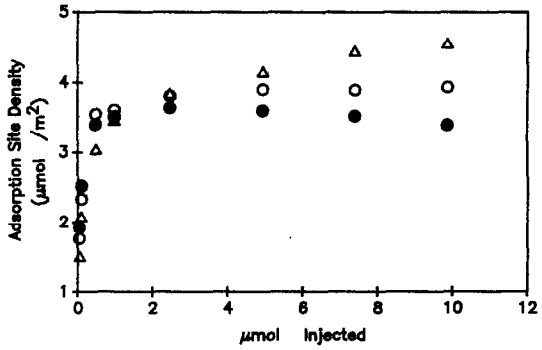

Fig. 4. Adsorption site densities for 3-phenyl-1-propanol as determined by the kinetic model using eqn. 16 (○), the Houghton equilibrium-dispersive model using eqn. 17a (●) and the Haarhoff–Van der Linde model using eqn. 18 (△). Experimental conditions are: flow-rate, 1.0 ml/min; mobile phase, methanol–water (25:75); temperature, 30.0°C; injection volume, 100 μl.

However, one interesting and potentially relevant observation which can be made is illustrated in Table III. In this table the physico-chemical parameters obtained upon injection of 0.02–2 μmol of 9-anthracenecarboxylic acid, under conditions for which it is completely ionized, are shown. The first point is that the same trend of peak width parameter *versus* loading is present for 9-anthracenecarboxylate as was observed for 3-phenyl-1-propanol in Table I. This indicates that this behavior is not limited to benzyl alcohol and its homologues. More significantly, however, the peak width is greater (*i.e.*, γ is lower; P and σ are higher) for 9-anthracenecarboxylate than for 3-phenyl-1-propanol (Table I) when compared on the basis of equal amounts injected. Jacobson *et al.*[20] observed that ionized solutes have column capacities nominally only a tenth that of comparable neutral solutes. In this work the carboxylate was observed to have only a fifteenth of the capacity of 3-phenyl-1-propanol (Table III). When 9-anthracenecarboxylate and 3-phenyl-1-propanol injections are compared on the basis of the degree of overload (*i.e.*, multiply 9-anthracenecarboxylate concentration by 15 for sake of comparison), it can be seen that the absolute value of the peak width parameters are approximately the same for the two solutes. Some discrepancy is to be expected due to the differences in k'. Thus, if it is assumed that the band broadening processes for the two solutes are the same, even though the factors controlling their isotherms are different, then the change in the peak width parameters is a function of the degree of column overload rather than the mobile phase solute concentration.

Obviously, more work needs to be done to elucidate the origin of this additional "overload induced" band broadening effect. Knowledge of the manner in which the overload increases the peak width parameters is an absolute prerequisite if any of the non-linear chromatography models are to be used to predict scale-up effects from linear chromatographic behavior.

An additional important observation from Table III is that the Haarhoff–Van der Linde model did not fit the experimental peak shape of the 2-μmol injection of 9-anthracenecarboxylate, as can be seen by the six-fold difference in the χ^2 between this model and the other two. Thus the Haarhoff–Van der Linde model can match experimental peak shapes under low or moderately overloaded peaks, whereas the

TABLE IV

EFFECT OF SOLUTE ON THE ADSORPTION SITE DENSITY ON A REVERSED-PHASE COLUMN

Conditions: injection volume, 100 μl; column temperature, 30.0°C; sample concentration, 0.05 *M* (except 9-anthracenecarboxylic acid); column, 150 × 4.6 mm I.D. C_{18} Vydak 201TPB (different column from Table V); flow-rate, 1.0 ml/min.

Solute	k'	γ	KC_0	Λ_0 ($\mu mol/m^2$)
2-Phenylethanol[a]	8.85	130	0.112	3.1
3-Phenyl-1-propanol[b]	10.46	190	0.108	3.7
4-Phenyl-1-butanol[c]	11.24	130	0.117	3.8
5-Phenyl-1-pentanol[d]	10.58	130	0.111	3.7
o-Cresol[a]	11.93	120	0.211	2.1
4-Ethylaniline[e]	10.96	270	0.058	6.5
9-Anthracenecarboxylic acid[f]	11.71	43	0.709	0.25

[a] Mobile phase methanol–water (10:90).
[b] Mobile phase methanol–water (25:75).
[c] Mobile phase methanol–water (31.5:68.5).
[d] Mobile phase methanol–water (40:60).
[e] Mobile phase methanol–phosphate buffer, pH 6.8 (25:75), with 0.010 *M* triethylamine.
[f] Sample concentration, 0.02 *M*; mobile phase methanol–phosphate buffer, pH 6.8 (20:80).

kinetic and Houghton equilibrium-dispersive models can match even severely overloaded chromatographic peaks.

Effect of flow-rate. The influence of flow-rate on the physico-chemical parameters of the three models is given in Table II for injections of 0.099 and 9.87 μmol of 3-phenyl-1-propanol. Overloading the column has the effect of shifting the *H versus u* plot upwards to higher plate heights, as observed previously[21,22], and shown in Fig. 2, where the open circles and open triangles correspond to the plate heights observed for injections of 0.099 and 9.87 μmol, respectively.

In essence, the band broadening due to overload of the isotherm can be separated from that of the linear chromatographic broadening processes:

$$H = H_{\text{linear}} + H_{\text{overload}} \tag{14}$$

This additivity of plate heights was first described by Haarhoff and Van der Linde[6] as a consequence of their model. A similar approximation can be made based on the kinetic model[23].

For injections of 0.099 μmol shown in Table II, the peak width parameters vary in the expected manner based on an *H–u* plot, since the loading is sufficiently low as to be on the linear portion of the isotherm. One can use the theory of linear chromatography to show that

$$H_{\text{linear}} = \frac{2k'}{(1+k')^2}\frac{L}{\gamma} \tag{15}$$

A plot of H_{linear} computed via the measured γ values for the 0.099 μmol injections is shown as the filled circles in Fig. 2. H_{linear} is slightly lower that the observed H since some of the band broadening was ascribed to the isotherm overload parameter (*i.e.*, KC_0 was not zero).

For the higher loading, 9.9 μmol, the chromatographic parameters are almost independent of flow-rate. The band broadening processes operative under trace conditions are still taking place; however, their effect on the peak width parameters is overwhelmed by the "solute overload effect" discussed in the last section. We also show the H_{linear} computed based on eqn. 15 and the measured value of γ (see Fig. 2, filled triangles). It is clear that we are now recovering a poorer value of γ since the peak width is dominated by the overload process. The observation that this "effect" is flow-rate independent is consistent with the assumption that it is related to the column overload, and not simply an enhancement of the traditional band broadening processes.

Similar results can be obtained using the peak width parameters of the Houghton and Haarhoff–Van der Linde models.

Overload parameters

In Table I, the effect of solute concentration on the overload parameters, KC_0, λC_0 and YC_0, is factored out, to yield K, λ and Y, which characterize the curvature of the isotherm at the origin. These isotherm parameters should be independent of concentration. For the 20-fold change in solute loading from 0.5 to 9.9 μmol: K decreases 12%, λ decreases 5% and Y decreases 30%. For lower amounts of solute, the system is essentially on the linear portion of the isotherm, and the isotherm parameters (K, λ, Y) respond to the minor peak asymmetry arising from effects other than isotherm overload (i.e., extra-column or dispersion effects). It is very difficult to measure the peak asymmetry at low overload. For instance the K observed for a 0.049-μmol injection of 3-phenyl-1-propanol was 82.6 M^{-1} (Table I, 1.0 ml/min). Generating a peak using the same k' and γ values but decreasing K to 36 M^{-1} (the value observed for a highly overloaded peak), resulted in only a 1% change in peak width and the peak asymmetry, as measured by the third statistical moment, varied from 0.0014 to 0.0008. The difference in χ^2 was insignificant.

The isotherm curvature at the origin is a rather esoteric parameter. The capacity of the column is a more useful and practical parameter. Jacobson *et al.*[20] found that the isotherms for a wide variety of solutes in reversed-phase chromatography were of the Langmuir form. Using this as the assumed isotherm form, the capacity of the column can be calculated using the isotherm parameters determined by each model. An expression for the column capacity, in terms of an adsorption site density. Λ_0 (μmol/m^2), has been derived[2]:

$$\Lambda_0 = \left(\frac{\varepsilon_T}{\rho a_S}\right)\left(\frac{k'}{K}\right) \tag{16}$$

where $\varepsilon_T = \varepsilon_e + \varepsilon_i(1 - \varepsilon_e)$. The interstitial ($\varepsilon_e$) and intraparticle ($\varepsilon_i$) porosities were both taken to be 0.4[24]; hence $\varepsilon_T = 0.64$. ρ is the density of the adsorbent in the packed tube, which was measured as 790 g/l. a_S is the specific surface area, which was measured

as 56 m^2/g by BET. C_0 is the concentration injected (in μM) times the fraction of the column dead volume represented by the 100-μl loop.

Using the same assumptions, the Houghton equilibrium-dispersive model yields the expression[19]:

$$\Lambda_0 = -\left[\frac{\varepsilon_T}{\rho a_S}\right]\left[\frac{2k'^2}{\lambda(1+k')}\right] \tag{17a}$$

where

$$\lambda = \frac{-2k'K}{1+k'} \tag{17b}$$

For the Haarhoff–Van der Linde model, the relevant expression is:

$$\Lambda_0 = \left(\frac{\varepsilon_T}{\rho a_S}\right)\left(\frac{2k'}{Y}\right) \tag{18}$$

Fig. 4 shows the adsorption site densities computed from each model for the data in Table I. All three models show essentially the same general trend. At low concentrations, where the peak skew results predominantly from factors other than isotherm overload, the adsorption site density appears to be low, since all of the models incorrectly attribute the other sources of peak asymmetry to the isotherm overload parameter. Once the isotherm overload effects become large enough to control the peak skew, the site densities approach a limiting value for the kinetic model, and drift downwards and upwards for the Houghton equilibrium-dispersive and the Haarhoff–Van der Linde models, respectively.

It is not correct to say that since the kinetic model gives reasonable results for the adsorption site density under high overload conditions, that overall the model is valid. At high sample loadings, the band is controlled mainly by the thermodynamic effect of overloading the column, not by kinetic effects. In fact, at moderate to high loadings, the ideal model[1] gives comparable results to the kinetic model for the adsorption site density. Thus the success of the kinetic model herein results solely from the asssumption of the correct form of the adsorption isotherm; the Langmuir isotherm.

The upward tendency of the site density calculated using the Haarhoff–Van der Linde model is not surprising, since the deviation between the parabolic isotherm used in the model and the Langmuir isotherm assumed in the derivation of eqn. 18 increases with increasing column overload. However, it is interesting that this deviation increases so rapidly after overload asymmetry becomes significant. This illustrates a shortcoming of both the Houghton and Haarhoff–Van der Linde equations. That is, their assumption that a parabolic isotherm is a reasonable approximation of the Langmuir isotherm is only valid at low overloads where the models are numerically not very sensitive to the value of the overload parameter.

With the Houghton equilibrium-dispersive model, the same deviation between the parabolic and Langmuir isotherms occurs, but the observed behavior is further

complicated by the lack of mass conservation inherent in this model. In a comparison of the kinetic and equilibrium-dispersive models, we observed that as the overload increased, λ deviated positively from its true value due to the mass loss[8]. Thus for the equilibrium-dispersive model, the deviation of its parabolic isotherm from the Langmuir is overwhelmed by the opposite effects arising from non-conservation of mass.

The adsorption site density for all three models is independent of flow-rate provided that the column is significantly overloaded. When 9.87 μmol of solute are injected (Table II), Λ_0 is 3.67 with a standard deviation of 0.08 μmol/m^2 for the kinetic model, 3.28 (0.07) for the Houghton equilibrium-dispersive model and 4.40 (0.09) for the Haarhoff–Van der Linde model.

The adsorption site densities determined for loadings greater than 1.0 μmol, 3.7 μmol/m^2, are in good agreement with the 4.3 μmol/m^2 observed for benzyl alcohol in methanol–water (30:70) determined using the Craig distribution model of non-linear chromatography[25], and it is also in reasonable agreement with the value expected for monolayer adsorption of the solute molecule (*ca.* 3 μmol/m^2) onto a collapsed ODS surface[26]. The fact that Λ_0 is close to the value expected based on an adsorption model of reversed-phase LC regardless of the model chosen is most interesting. It is not evident how a partition model of reversed-phase LC could lead to such a coincidence.

Effect of mobile phase on adsorption site density. As shown above, only the adsorption site density derived from the kinetic model is independent of both the amount of solute and flow-rate. While this behavior and the value of Λ_0 for 3-phenyl-1-propanol are consistent with expectations, it still remains to be shown that this parameter has any physical significance. Shown in Table V are the physico-chemical parameters obtained from fits of the kinetic model to additional experiments in which 5 μmol of 3-phenyl-1-propanol were injected under various mobile phase conditions. Using mobile phases of between 15 and 35% methanol, the adsorption site density, as calculated from eqn. 16, is constant; at methanol–water (10:90), Λ_0 drops by 20%. Previously, Jaulmes *et al.*[19] studied a similar system (benzyl alcohol) in 10–30% methanol using the Houghton equilibrium-dispersive model; but uncertainties in their measurements obscured any such trend. Eble *et al.*[26], using the Craig distribution model, observed a constant (within experimental error) capacity for benzyl alcohol over the range of 20 to 40% methanol, although they did comment that there may be a small increase associated with increasing modifier concentration in the mobile phase[25].

The behavior of Λ_0 observed for methanol–water mobile phase can be rationalized in terms of the wetting characteristics of reversed-phase bonded phases. McCormick and Karger[27] observed that the amount of methanol sorbed by an octyl stationary phase increased for mobile phase concentrations of methanol up to 20% and was constant for higher concentrations of methanol. The sorption of methanol into the collapsed bonded phase will solvate the octyl chains, allowing them to adopt more of a "brush" orientation[28]. We believe that the "brush" orientation exposes a larger surface of the octyl chains than does a collapsed chain, which then becomes available to interact with the solute, and thus producing a higher effective site density.

In Table V, the data for the tetrahydrofuran (THF)–water system indicate a capacity comparable to the well methanol-wetted stationary phase, and increasing the percentage of THF makes a small, but significant, change in the adsorption site

TABLE V

EFFECT OF MOBILE PHASE ON ADSORPTION SITE DENSITY FOR 3-PHENYLPROPANOL

Conditions: injection volume, 100 μl; column temperature, 30.0°C; sample concentration, 0.05 *M*; column, 150 × 4.6 mm I.D. C_{18} Vydak 201TPB; flow-rate, 1 ml/min. All experiments, except methanol–water (10:90), were run successively.

Mobile phase	k'	γ	KC_0	Λ_0 ($\mu mol/m^2$)
Methanol–water (10:90)[a]	25.35	48	0.334	2.9
Methanol–water (15:85)	21.86	59	0.232	3.6
Methanol–water (25:75)	10.06	160	0.102	3.7
Methanol–water (35:65)	4.45	300	0.045	3.7
THF–water (10:90)	8.66	180	0.089	3.7
THF–water (15:85)	5.40	280	0.052	3.9

[a] Column was a second 150 × 4.6 mm I.D. C_{18} Vydak 201TPB column.

density. This result is consistent with the THF isotherm behavior on octyl bonded phases[27], where it was observed that the isotherm did not level off until 40–60% THF. However it is surprising that the use of the much stronger modifier, THF, had such a small effect on the capacity. This indicates that the major capacity effect of the modifier is to solvate the bonded phase such that it can adopt the "brush" form. Once the bonded phase is in the brush form, further increases in mobile phase do not significantly alter its form, and thereby its capacity.

Effect of solute type on adsorption site density. The physico-chemical parameters obtained by fitting the kinetic model to injections of a number of chemically distinct solutes are shown in Table IV. It should be noted that a different column, but packed with the same stationary phase, was used in this experiment than in Table V. Nevertheless, Λ_0 for 3-phenyl-1-propanol is still the same as for the column used in the previous studies (Table V). The larger benzyl alcohol homologues show similar adsorption site densities to 3-phenyl-1-propanol, but 2-phenylethanol was significantly lower. However, this lower value of Λ_0 is probably a result of wetting the stationary phase, as is evident by comparing Λ_0 for 2-phenylethanol with 3-phenyl-1-propanol in methanol–water (10:90) (Table V).

Other types of solutes show strikingly different adsorption site densities from that of the benzyl alcohol homologues. *o*-Cresol shows a lower capacity than 3-phenyl-1-propanol under the same mobile phase conditions [2.1 *vs.* 2.9 $\mu mol/m^2$ for methanol–water (10:90)]. This is comparable to the relationship observed recently by Golshan-Shirazi and Guiochon[1] for phenol and benzyl alcohol. In contrast 4-ethylaniline has a capacity 1.75 times greater than that of 3-phenyl-1-propanol. This is consistent with the results of Jacobson *et al.*[20], in which the capacity of *p*-toluidine (4-methylaniline) was 2.74 times that of phenol on ODS using pure water as the mobile phase. It should be noted that 4-ethylaniline is silanophilic, but if it had been strongly retained by the silanols, the peak would have been more tailed and the model would then have predicted a low capacity rather than the higher capacity observed. Finally, 9-anthracenecarboxylate has an adsorption site density of only 0.25 $\mu mol/m^2$. Such low capacities are typical of ionized solutes[20].

Thus, the behavior of the adsorption site density, and therefore K, derived from the kinetic model, is consistent with previous observations and rational expectations.

CONCLUSIONS

A good fit between a non-linear chromatographic model and experimental overloaded peaks cannot be used as the sole criterion of a model's validity. The kinetic, Houghton equilibrium-dispersive and Haarhoff–Van der Linde models all precisely reproduce the peak shapes observed under low to moderate overload conditions. However for all of the models the parameter which describes the peak width under linear chromatographic conditions, and thus should be independent of solute concentration, was found to vary several fold as the extent of column overload was increased. Since the models were derived using distinctly different assumptions, it is believed that this parameter variation results from a physical band broadening process intrinsic to the overloading of the column. The origin of this additional band broadening process is as yet unknown, but is a question which warrants further investigation.

Another conclusion from this work is that the isotherm parameter of the equilibrium-dispersive and Haarhoff–Van der Linde model lacks physical significance as the result of the intrinsic assumption of an unrealistic isotherm. The former model also is affected by the effects of a mathematic failure to conserve mass. The isotherm parameter of the kinetic model, and the associated adsorption site density, do appear to have physical significance. The adsorption site density derived from this model does not vary with solute concentration, when the skew due to column overload is significant. Also, the variation of the site density with mobile phase and solute is consistent with results from traditional breakthrough studies. These results indicate that the kinetic model may be a convenient method of studying factors affecting the capacity of high-performance liquid chromatography packings. Studies such as those described here are much faster than breakthrough curve studies and provide more detailed information at the cost of some computational complexity.

Finally, we believe that the data indicate there is, at present, no model which incorporates all of the important events involved in retention in reversed-phase LC.

ACKNOWLEDGEMENTS

This work was supported in part by grants from the Institute for Advanced Studies in Biological Process Technology, University of Minnesota, and the 3M Company. Charles Lucy was supported by a fellowship from the Natural Science and Engineering Research Council of Canada. We also would like to thank Professor Abraham Lenhoff for his comments during the course of this work.

REFERENCES

1 S. Golshan-Shirazi and G. Guiochon, *Anal. Chem.*, 61 (1989) 462.
2 J. L. Wade, A. F. Bergold and P. W. Carr, *Anal. Chem.*, 59 (1987) 1286.
3 H. C. Thomas, *J. Am. Chem. Soc.*, 66 (1944) 1664.
4 G. Houghton, *J. Phys. Chem.*, 67 (1963) 84.
5 A. Jaulmes, C. Vidal-Madjar, H. Colin and G. Guiochon, *J. Phys. Chem.*, 90 (1986) 207.
6 P. C. Haarhoff and H. J. van der Linde, *Anal. Chem.*, 38 (1966) 573.

7 G. Cretier and J. L. Rocca, *Chromatographia*, 18 (1984) 623.
8 J. L. Wade and P. W. Carr, *J. Phys. Chem.*, submitted for publication.
9 J. C. Giddings, *Dynamics of Chromatography*, Part I, Marcel Dekker, New York, 1965.
10 N. K. Hiester and T. Vermeulen, *Chem. Eng. Prog.*, 48 (1952) 505.
11 M.-S. Razavi, B. J. McCoy and R. G. Carbonell, *Chem. Eng. J.*, 16 (1978) 211.
12 J. B. Rosen, *J. Phys. Chem.*, 20 (1952) 387.
13 R. S. Cooper and D. A. Liberman, *Ind. Eng. Chem. Fundam.*, 9 (1970) 620.
14 R. S. Cooper, *Ind. Eng. Chem. Fundam.*, 4 (1965) 308.
15 K. R. Hall, A. Acrivos, L. C. Eagleton an T. Vermeulen, *Ind. Eng. Chem. Fundam.*, 5 (1966) 212.
16 H. Poppe and J. C. Kraak, *J. Chromatogr.*, 255 (1983) 395.
17 J. C. Giddings and H. Eyring, *J. Phys. Chem.*, 59 (1955) 416.
18 J. L. Wade, *Ph.D. Thesis*, University of Minnesota, Minneapolis, MN, 1988.
19 A. Jaulmes, M. J. Gonzalez, C. Vidal-Madjar and G. Guiochon, *J. Chromatogr.*, 387 (1987) 41.
20 J. Jacobson, J. Frenz and Cs. Horváth, *J. Chromatogr.*, 316 (1984) 53.
21 A. W. J. de Jong, J. C. Kraak, H. Poppe and F. Nooitgedacht, *J. Chromatogr.*, 193 (1980) 181.
22 C. Dewaele, M. de Coninck and M. Verzele, *Sep. Sci. Technol.*, 22 (1987) 1919.
23 C. A. Lucy and P. W. Carr, in preparation.
24 K. K. Unger, J. N. Kinkel, B. Anspach and H. Giesche, *J. Chromatogr.*, 296 (1984) 3.
25 J. E. Eble, R. L. Grob, P. E. Antle and L. R. Snyder, *J. Chromatogr.*, 405 (1987) 31.
26 J. E. Eble, R. L. Grob, P. E. Antle and L. R. Snyder, *J. Chromatogr.*, 384 (1987) 45.
27 R. M. McCormick and B. L. Karger, *Anal. Chem.*, 52 (1980) 2249.
28 R. K. Gilpin, *J. Chromatogr. Sci.*, 22 (1984) 371.